ChemComm

RSC Publishing

COMMUNICATION

View Article Online
View Journal | View Issue

Cite this: *Chem. Commun.*, 2013, **49**, 11400

Received 18th September 2013,
Accepted 10th October 2013

DOI: 10.1039/c3cc47138a

www.rsc.org/chemcomm

Fast, single-step, and surfactant-free oligonucleotide modification of gold nanoparticles using DNA with a positively charged tail†

Ron Gill,*[a] Kristian Göeken[a] and Vinod Subramaniam[ab]

Fast modification of large gold nanoparticles with DNA is achieved by using DNA with a polycationic tail. The conjugated DNA is available for specific hybridization, and therefore can be used for DNA-based assays or for constructing nanoparticle superstructures based on DNA hybridization.

Within the toolbox of nanoscience, organic–inorganic hybrid nanoparticles make up one of the most versatile groups of functional nanoparticles. Specifically, DNA-coated gold nanoparticles have attracted particularly high interest from the research community since the pioneering work of Mirkin *et al.*[1] These particles have found a wide range of applications, from biosensing[2,3] and drug delivery[4,5] to the construction of photonic crystals.[6,7] A prerequisite for all these applications is the stable modification of the nanoparticles. As gold nanoparticles are usually synthesized using a negatively charged ligand (such as citrate or tannic acid) and DNA is also negatively charged, a high salt concentration is needed to promote the attachment of the DNA to the nanoparticles. However unmodified nanoparticles are not colloidally stable under high salt conditions. Therefore the most commonly reported modification method, which is referred to as 'the salt aging' method, involves the slow addition of a salt over several hours to days.[1] Alternatively, slow evaporation of the solvent will also cause a gradual increase of the salt concentration with time, leading to stable modification of the nanoparticles.[8] In recent years several faster methods have been introduced, taking the process duration down to a couple of hours by using surfactants to stabilize the nanoparticles during the salt addition.[9,10] However the use of surfactants can complicate downstream applications, for example in microfluidic devices. Very recently, a rapid 5 minute, two-step modification procedure has been reported, which can be used to modify both gold[11] and silver[12] nanoparticles. This procedure is based on the fact that A and C bases are positively charged at low pH, thus allowing fast modification of DNAs using acidic citrate buffer at pH = 3. However, this method still has disadvantages. The use of DNA bases to create a positively charged tail can lead to complications if the recognition DNA sequence has a high A/C stretch in it. Furthermore, we observed that larger nanoparticles (*i.e.* $\geq$40 nm diameter) are less stable in the citrate buffer than smaller particles, and therefore need either longer incubation time at pH = 7 or modification at very high concentrations.[13]

Here we report on the development of a single-step, surfactant-free method that leads to the modification of salt stable particles within minutes, Fig. 1. This method works even with the challenging larger (40 nm and 80 nm in diameter) gold nanoparticles. This result was achieved by replacing the conventional thiol-terminated DNA with a polyspermine-terminated DNA commercially known as Zip Nucleic Acid (ZNA).[14] Additionally we show that using a conventional UV-VIS spectrometer, the kinetics of DNA adsorption can be followed with time, and the effects of the experimental conditions, such as the salt concentration in the buffer, can be studied.

As a first proof of principle for this method, we chose the modification of moderately large, 40 nm diameter gold nanoparticles, which is more challenging compared to smaller particles (20 nm in diameter and less). We have recently shown[13] that for such particles, at typical commercially supplied concentrations (0.005% Au by wt), salt stable modification cannot be achieved within 5 minutes for a low excess of DNA using the acidic citrate buffer method. The ZNA probes we use

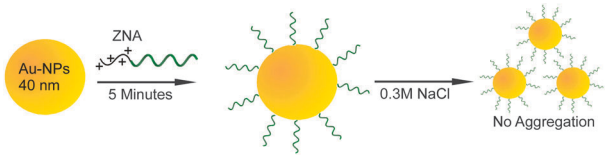

Fig. 1 ZNA attachment to 40 nm gold particles results in salt stable particles after just 5 minutes of incubation.

[a] *Nanobiophysics Group, MIRA Institute of Biomedical Technology and Technical Medicine, University of Twente, Enschede, The Netherlands. E-mail: r.gill@utwente.nl; Fax: +31 53489 1105; Tel: +31 53489 3067*
[b] *FOM Institute AMOLF, Science Park 104, 1098 XG, Amsterdam, The Netherlands*

† Electronic supplementary information (ESI) available: Materials and methods, DLS measurements, and the UV-VIS absorbance spectrum of 80 nm gold nanoparticles modified with ZNA. See DOI: 10.1039/c3cc47138a

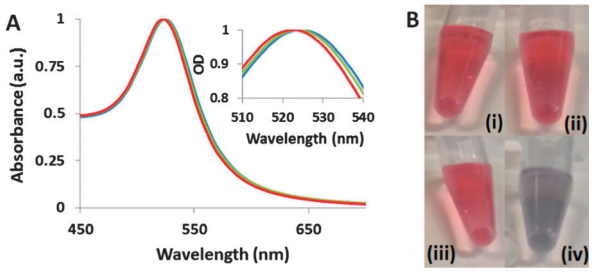

Fig. 2 (A) UV-VIS absorption spectra of gold nanoparticles before (red), after the addition of DNA (green) and after the addition of a salt (blue). The inset shows a magnification of the absorbance peak. (B) Photographs of gold nanoparticles after incubation with DNA and addition of a salt. The DNA sequences used were (i) ZNA-cap, (ii) tag-ZNA, (iii) ZNA-polyT, and (iv) HS-5A-cap.

are comprised of three parts: a positively charged tail, which promotes the attachment of the DNA to the nanoparticle; a 5T spacer, chosen because T bases were shown[15,16] to have the least affinity for gold; and a DNA capture sequence, which can be used in downstream applications for specific hybridization. In a typical experiment, 1 μl of 100 μM ZNA-cap (see ESI† for sequence details) was mixed with 1 ml of gold nanoparticles (40 nm in diameter). After 5 minutes, a 500 μl aliquot was transferred to a new Eppendorf tube and mixed with 200 μl of 1 M NaCl, leading to a solution with a final concentration of ~0.3 M NaCl. No color change associated with aggregation was observed, and no red shoulder in the absorbance spectrum was detected, Fig. 2. The lack of aggregation is also supported by dynamic light scattering (DLS) measurements (see Fig. S1 in the ESI†). This is in contrast to the same sequence with a thiol instead of the ZNA tail (HS-cap), which did not protect the gold nanoparticles from aggregation upon the addition of NaCl, Fig. 2B.

We observed that using both the salt aging method and the acidic citrate methods, functionalization with DNA that has a 3′-modification (*i.e.* thiol) is more difficult than with 5′-modified sequences, and usually requires a higher excess of DNA to achieve salt-stable particles. In order to test whether the modification with ZNA is also sensitive to the position at which the positively charged tail is attached, we attempted the modification of the nanoparticles with the tag-ZNA sequence that has the poly-spermine tail at the 3′-end rather than at the 5′-end of the DNA sequence. As can be seen in Fig. 2B, no aggregation occurred after salt addition, although we used the same low excess (1.5× compared to maximum theoretical DNA coverage) and short incubation time (5 minutes).

To demonstrate the versatility of our ZNA-based method compared to modification using the acidic citrate buffer method, the particles were modified with a poly T sequence (ZNA-PolyT). Particles modified with a poly T sequence are often used to capture mRNAs that naturally contain a poly A sequence at the 3′-end.[17] As the thymine base is not protonated at pH = 3, effective modification with a poly T sequence cannot be achieved by the acidic citrate buffer method,[18] however, as can be seen in Fig. 2B, using a ZNA tail, fast salt stable modification is achievable for a poly T sequence. Attempting to modify even larger, 80 nm diameter particles using the described protocol was also successful (see Fig. S2 in the ESI†).

During our experiments with ZNA we observed that our modification procedure would fail, both when using nanoparticles that were diluted in water and using commercial particles that were supplied suspended in water (in the absence of buffer and salt). In order to investigate the effect of the buffer and salt concentration at which the reaction takes place, we have developed a procedure for directly following the kinetics of the DNA binding reaction.

Kinetics of thiol adsorption on gold surfaces have been measured more than a decade ago using a quartz crystal microbalance (QCM).[19] For nanoparticle modification, most authors have published results based on fluorescence quenching of fluorophores as they come into proximity of the gold nanoparticles. However quenching measurements can be complicated by fluorescence bleaching processes and adsorption on the side walls. Additionally, pH dependence of fluorophores can limit *in situ* measurements of the binding kinetics, as was the case in the acidic citrate method, where sampling at different time points had to be used. The direct observation of binding kinetics using the shift of the localized surface plasmon resonance (LSPR) peak is usually considered technically challenging, as the total shift is in the range of 1–2 nm, raising the need for sub-0.1 nm resolution. To overcome this challenge we have employed a method that has so far been applied mainly to surface-based LSPR sensors, namely the fitting of the full spectral data to calculate the position of the maxima of scattering/extinction with high accuracy. Although several advanced algorithms were published,[20,21] we found that a simple fit of the top of the plasmon peak with the Lorentzian fitting function in MATLAB was sufficient to generate high quality, low noise (<0.01 nm noise level) kinetics data.

Fig. 3A shows a representative kinetic curve of the plasmon peak shift with time after the addition of the ZNA-cap to gold nanoparticles. As can be seen in the graph, the maximum shift reached is about 1.3 nm, and the shift after 5 minutes is very close to the saturation level. The inset shows the noise level as measured by taking 20 consecutive measurements every 30 seconds. The absolute noise level in these measurements is very low, and the particles are stable (*i.e.* no noticeable drift in the peak position over time).

With this tool in hand we went on to examine the effect of buffer and salt concentration. The graph in Fig. 3A was

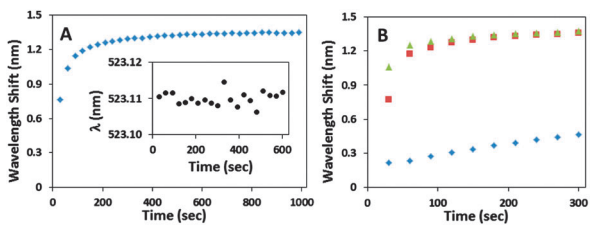

Fig. 3 (A) Time dependence of the shift in the position of the plasmon peak absorbance, upon incubation of 40 nm gold nanoparticles (from Nanocomposix) with ZNA. Inset – stability of the position of the plasmon peak absorbance with time for 40 nm gold nanoparticles. (B) Time dependence of the shift of the position of the plasmon peak absorbance upon incubation of 40 nm gold nanoparticles (from BBI) with ZNA, when the particles were suspended in water (diamonds), 6 mM NaCl (squares) or 2 mM Na_3Cit (triangles).

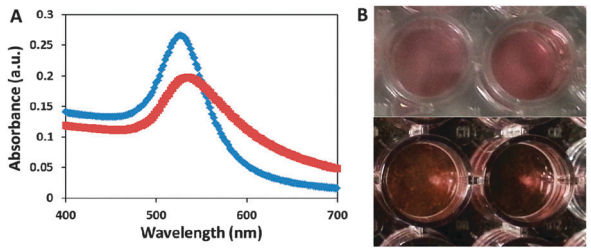

Fig. 4 (A) UV-Vis spectra of a mixture containing ZNA-cap coated gold nanoparticles, tag-ZNA gold nanoparticles and either a target which is complementary to both strands (Targ1, red squares) or a non-complementary target (NST, blue diamonds). (B) Photographs of the gold nanoparticles after incubation with the complementary target strand (left) or non-complementary target (right). The bottom photograph is the same wells, pictured with a dark background.

measured for commercial nanoparticles (from Nanocomposix, USA) that are dispersed in a 2 mM Na_3Cit buffer. These particles are the same as the ones shown in Fig. 2A, which shows that 5 minutes of incubation were enough to stabilize the particles against aggregation in $\sim$0.3 M NaCl. On the other hand, commercial nanoparticles that are dispersed in water (from BBI, UK) aggregated during the salt addition step of our protocol. However, this problem could be overcome by addition of either Na_3Cit buffer to a 2 mM final concentration, or even by addition of NaCl to a 6 mM final concentration, both of which produced salt stable nanoparticles after 5 min of reaction with the ZNA-cap.

These results are supported by the kinetics measurements we did on these three systems, Fig. 3B. For the sample with the nanoparticles in water, slower kinetics were observed, and the total shift of the plasmon peak after 5 minutes was also smaller compared to Fig. 3A. However, addition of 6 mM of Na^+ ions either in the form of 2 mM Na_3Cit or in the form of 6 mM NaCl resulted in comparable kinetics and the total LSPR peak shift to those shown in Fig. 3A. We therefore conclude that the cation concentration in the solution plays a major role in both the kinetics of the adsorption and the final capacity (no. of ZNA-caps per particle). These results show a similar influence of the salt concentration as those observed previously with DNA modification of gold nanoparticles.[12] However, due to the much lower total charge of the ZNA, the effect is observed at about 10$\times$ lower salt concentration.

In order to test whether ZNA-functionalized gold particles are capable of specific hybridization, we combined ZNA-cap functionalized particles with tag-ZNA functionalized particles, in the presence of the target sequence 'Targ1' (complementary to both sequences and therefore promoting aggregation of the particles) or the non-specific target 'NST'. As can be seen in Fig. 4A, a significant increase in the absorbance between 600 nm and 700 nm is observed for the sample that contained the target. Although a slight shift toward purple can be seen by eyes (Fig. 4B, top), the difference between the aggregated and non-aggregated samples can be visualized much better by looking specifically at the scattering component, which can be seen when using a dark background (Fig. 4B, bottom).

In summary, we have demonstrated that fast (5 min), stable modification of large gold nanoparticles with a DNA sequence could be achieved using DNA sequences with a cationic tail, commercially available as ZNAs. The modified particles were stable at high salt concentrations, and the DNA on the particle retained its functional ability for specific hybridization.

The work of R. G. has been funded by an NWO Veni grant (No. 700.10.410).

Notes and references

1 C. A. Mirkin, R. L. Letsinger, R. C. Mucic and J. J. Storhoff, *Nature*, 1996, **382**, 607–609.
2 R. Elghanian, J. J. Storhoff, R. C. Mucic, R. L. Letsinger and C. A. Mirkin, *Science*, 1997, **277**, 1078–1081.
3 L. He, M. D. Musick, S. R. Nicewarner, F. G. Salinas, S. J. Benkovic, M. J. Natan and C. D. Keating, *J. Am. Chem. Soc.*, 2000, **122**, 9071–9077.
4 N. L. Rosi, D. A. Giljohann, C. S. Thaxton, A. K. R. Lytton-Jean, M. S. Han and C. A. Mirkin, *Science*, 2006, **312**, 1027–1030.
5 P. Ghosh, G. Han, M. De, C. K. Kim and V. M. Rotello, *Adv. Drug Delivery Rev.*, 2008, **60**, 1307–1315.
6 S. Y. Park, A. K. R. Lytton-Jean, B. Lee, S. Weigand, G. C. Schatz and C. A. Mirkin, *Nature*, 2008, **451**, 553–556.
7 D. Nykypanchuk, M. M. Maye, D. van der Lelie and O. Gang, *Nature*, 2008, **451**, 549–552.
8 A. G. Kanaras, Z. Wang, A. D. Bates, R. Cosstick and M. Brust, *Angew. Chem., Int. Ed.*, 2003, **42**, 191–194.
9 S. I. Stoeva, J.-S. Lee, C. S. Thaxton and C. A. Mirkin, *Angew. Chem., Int. Ed.*, 2006, **45**, 3303–3306.
10 Y. Zu and Z. Gao, *Anal. Chem.*, 2009, **81**, 8523–8528.
11 X. Zhang, M. R. Servos and J. Liu, *J. Am. Chem. Soc.*, 2012, **134**, 7266–7269.
12 X. Zhang, M. R. Servos and J. Liu, *Chem. Commun.*, 2012, **48**, 10114–10116.
13 X. Zhang, T. Gouriye, K. Göeken, M. R. Servos, R. Gill and J. Liu, *J. Phys. Chem. C*, 2013, **117**, 15677–15684.
14 V. Moreau, E. Voirin, C. Paris, M. Kotera, M. Nothisen, J.-S. Rémy, J.-P. Behr, P. Erbacher and N. Lenne-Samuel, *Nucleic Acids Res.*, 2009, **37**, e130.
15 J. J. Storhoff, R. Elghanian, C. A. Mirkin and R. L. Letsinger, *Langmuir*, 2002, **18**, 6666–6670.
16 L. K. Wolf, Y. Gao and R. M. Georgiadis, *Langmuir*, 2004, **20**, 3357–3361.
17 M. Huber, T.-F. Wei, U. R. Müller, P. A. Lefebvre, S. S. Marla and Y. P. Bao, *Nucleic Acids Res.*, 2004, **32**, e137.
18 X. Zhang, B. Liu, N. Dave, M. R. Servos and J. Liu, *Langmuir*, 2012, **28**, 17053–17060.
19 D. S. Karpovich and G. J. Blanchard, *Langmuir*, 1994, **10**, 3315–3322.
20 A. B. Dahlin, J. O. Tegenfeldt and F. Höök, *Anal. Chem.*, 2006, **78**, 4416–4423.
21 G. Raschke, S. Kowarik, T. Franzl, C. Sönnichsen, T. A. Klar, J. Feldmann, A. Nichtl and K. Kürzinger, *Nano Lett.*, 2003, **3**, 935–938.